Linking runoff and erosion dynamics to nutrient fluxes in a degrading dryland landscape

Katerina Michaelides,[1] Debbie Lister,[1,2] John Wainwright,[3] and Anthony J. Parsons[4]

Received 10 May 2012; revised 17 September 2012; accepted 18 September 2012; published 2 November 2012.

[1] Current theories of land degradation assume that shifts in vegetation communities result in changes to the rates and patterns of water and sediment movement, which are vectors of nutrient redistribution. This nutrient redistribution is hypothesized to reinforce, through positive feedbacks, progressive vegetation changes toward a more degraded ecosystem. A key component of this theory, which is currently poorly resolved, is the relative role of runoff and erosion in driving nutrient fluxes from different vegetation types. We address this gap through a series of field-based, rainfall-simulation experiments designed to explore plant-level dynamics of runoff- and erosion-driven nutrient fluxes of N, P and K species. Our results highlight important linkages between physical and biogeochemical processes that are controlled by plant structure. We found that: 1) the magnitude of sediment-bound nutrient export is determined by the grain-size distribution of the eroded sediment and the total sediment yield; 2) the partitioning of nutrients in dissolved and sediment-bound form is determined by the availability and concentration of different nutrient species in the soil or rainfall; 3) these processes varied according to vegetation type and resulted in stark differences between degrading and invading plant communities. Specifically, we observed that grassland areas consistently exported the highest yields of sediment-bound N, P and K despite producing similar erosion rates to shrub and intershrub areas. Our results have implications for better understanding how grassland areas are being replaced by shrubs and provide insights into the mechanisms of continuing land degradation in drylands.

Citation: Michaelides, K., D. Lister, J. Wainwright, and A. J. Parsons (2012), Linking runoff and erosion dynamics to nutrient fluxes in a degrading dryland landscape, *J. Geophys. Res.*, *117*, G00N15, doi:10.1029/2012JG002071.

1. Introduction

[2] Degrading dryland landscapes undergo significant ecosystem transformations associated with progressive changes in the dominant vegetation communities [*Schlesinger et al.*, 1990]. Regardless of the original cause of these vegetation shifts (anthropogenic, climatic), the resulting landscape changes—physical, structural and biological—can be significant. Existing theories on landscape-degradation dynamics suggest that the long-term and irreversible ecosystem shifts over centennial to millennial timescales result from complex feedbacks that arise between vegetation type, water and sediment transfers, and the associated nutrient fluxes, such that some vegetation communities are able to persist and expand over others [*Okin et al.*, 2009; *Schlesinger et al.*, 1990; *Turnbull et al.*, 2008].

[3] A particular example of a landscape exhibiting ongoing land degradation is the southwest USA, which has seen a progressive shift in dominant vegetation species from perennial grassland to woody shrubland over the last 150 years. Extensive research has shown that once established, shrubs autogenically out-compete grasses through accumulation of nutrients in sediment mounds beneath their canopies, creating localized "islands of fertility" [*Charley and West*, 1975; *Schlesinger et al.*, 1990, 1996]. This process not only increases the spatial heterogeneity of nutrients in the landscape [*Schlesinger et al.*, 1996], but also alters the microtopography and soil-surface characteristics, which impact on the redistribution of water and sediment [*Wainwright et al.*, 2002]. Whereas grassland areas typically have uniform vegetation cover and subdued microtopography, shrublands are characterized by patchy vegetation interspersed with bare areas (intershrubs) and have high relief microtopography due to the progressive formation of fertile mounds beneath the shrubs [*Parsons et al.*, 1996; *Wainwright et al.*, 2000].

[4] Changes in the spatial heterogeneity and type of vegetation lead to pronounced alterations to the spatial patterns

[1]School of Geographical Sciences, University of Bristol, Bristol, UK.
[2]Now at Eunomia Research and Consulting, Bristol, UK.
[3]Science Laboratories, Department of Geography, Durham University, Durham, UK.
[4]Sheffield Centre for International Drylands Research, Department of Geography, University of Sheffield, Sheffield, UK.

Corresponding author: K. Michaelides, School of Geographical Sciences, University of Bristol, University Road, Bristol BS8 1SS, UK. (katerina.michaelides@bristol.ac.uk)

0148-0227/12/2012JG002071

and biogeochemical cycling of soil nutrients [*Cross and Schlesinger*, 1999; *Schlesinger et al.*, 1996], the most important for vegetation being nitrogen (N), phosphorus (P) and potassium (K). The changes in microtopography and soil-surface properties that accompany shifts in vegetation from grassland to shrubland also result in landscape structural changes, which affect the redistribution of overland flow and sediment [*Parsons et al.*, 1996, 2003; *Wainwright*, 2009]. Theories on the continuing degradation of drylands have focused on feedbacks between the structural and ecological transformation of the landscape, biogeochemical patterns, and the redistribution of nutrients driven by wind and water [*Aguiar and Sala*, 1999; *Breshears et al.*, 2003; *Li et al.*, 2007, 2008; *Okin et al.*, 2009; *Ravi et al.*, 2007]. Understanding these linkages between transport vectors and nutrient relocation within vegetation communities has implications for the relative importance of: aeolian versus water-driven processes; changing ecosystem structure on nutrient sources and sinks; and the connections between nutrient transfers at different scales.

[5] Research has shown that rainfall-driven runoff and erosion are potentially significant processes in the sequence of feedbacks that drive land degradation [*Aguiar and Sala*, 1999; *Michaelides et al.*, 2009; *Mueller et al.*, 2007; *Parsons et al.*, 2003; *Schlesinger et al.*, 1990; *Wainwright et al.*, 2000, 2002]. During the infrequent but often extreme rainfall events that occur in many dryland environments, runoff can transport and redistribute significant quantities of nutrients within vegetation communities [*Brazier et al.*, 2007; *Parsons et al.*, 2003; *Schlesinger et al.*, 1999, 2000; *Turnbull et al.*, 2010, 2011], thereby maintaining or accentuating ecosystem shifts toward the vegetation communities that are nutrient sinks. Despite the well acknowledged role of erosion in the land degradation process, and the well documented significance of particulate forms of nutrients on watershed- and global-scale biogeochemical cycles [*Fierer and Gabet*, 2002; *Gabet et al.*, 2005; *Meybeck*, 1982; *Schlesinger et al.*, 1990], sediment-bound nutrient fluxes during erosion events and their impact on land degradation remain poorly understood in drylands [*Schlesinger et al.*, 1999; *Turnbull et al.*, 2011].

[6] This research investigates the linkages between the physical drivers of runoff and erosion and the nutrient fluxes they produce. We specifically focus on the relative partitioning of N, P, K nutrient species between the dissolved phase in the runoff and the sediment-bound phase transported on the eroded sediment, from plant-scale plots within different vegetation communities. The aim is to explore how the interactions between vegetation type, runoff and erosion, affect relative nutrient losses from the predominant vegetation communities and to examine how these dynamics may impact land degradation at the landscape scale. We use a series of rainfall-simulation experiments to investigate the runoff and erosion response from different vegetation types, and we quantify the N species (NH_4-N, NO_3-N, NO_2-N, TN), P species (PO_4-P, TP) and exchangeable K^+ dissolved in the runoff and adsorbed on different particle-size fractions of the eroded sediment. A comprehensive analysis of the partitioning of nutrients in runoff and on eroded sediment at the plant level is important for gaining new understanding of the potential export of bio-essential nutrients from different vegetation communities.

2. Study Area

[7] The Jornada Basin (32°31′N, 106°47′W) is situated ca. 40 km NNE of Las Cruces, New Mexico, USA. The climate is semi-arid to arid with a mean annual precipitation of 245 mm and a mean annual potential evapotranspiration of 2204 mm. The precipitation regime is characterized by intense, short-duration, convective summer storms [*Wainwright*, 2006]. Dominant shrubland species of the region are creosotebush (*Larrea tridentata*), honey mesquite (*Prosopis glandulosa*) and tarbush (*Flourensia cernua*). These shrub species have steadily increased since the 1850s and have replaced large areas of black grama grass (*Bouteloua eriopoda*) and other grasses [*Buffington and Herbel*, 1965; *Gibbens et al.*, 2005]. The Jornada Basin has seen an increase in the dominance of the mesquite shrub from 11% in 1938 to more than 37% in 1998. In addition, areas of the creosotebush shrub increased from 40% to 46% over the same time period while in contrast, the areas of grassland decreased from 26% coverage to 7% [*Gibbens et al.*, 2005]. Reasons for such changes in vegetation have been cited as a combination of climate change, grazing by livestock and plant competition for available space, moisture and nutrients [*Whitford*, 2002], and because of interactions of factors at local levels [*Yao et al.*, 2006].

[8] Study sites were situated within communities of mesquite, black grama grassland and creosotebush, located on the bajada slopes of Summerford Mountain, a rocky inselberg at the northern tip of the Doña Ana Mountains mostly composed of quartz monzonite with localized rhyolites. The monzonite rock contains apatite, a group of phosphate minerals which, when weathered, generate phosphates, the most common forms of which are the ions $H_2PO_4^-$ and HPO_4^{2-} [*Newman*, 1995]. Calcite has also been found to be abundant in the soils of the Jornada Basin [*Kraimer et al.*, 2005], despite the lack of limestone in the study area. Sources of calcite include aeolian sediments, rainfall [*Monger et al.*, 2006; *Schlesinger*, 1985], and the weathering of calcium feldspars and apatite within the monzonite rock [*Kraimer et al.*, 2005]. The bajada is made up mainly of igneous alluvial deposits derived from the igneous rocks of Summerford Mountain with a contribution of sandy deposits from the ancestral and present Rio Grande. The surface horizon texture of these soils consists of sandy loams or loamy sands and contains variable amounts of gravel on the surface as erosional lags. Soils are classified as Typic Haplargids and Torriorthentic Haplustolls with localized Typic Haplocalcids [*Gile et al.*, 1997; *Monger*, 2006]. Mesquite shrubs occur predominantly in the eastern and central part of the Jornada Basin while the creosotebush shrubs are more predominant within the lower and upper piedmont slopes of the Basin. Black grama grasslands occur typically on upland slopes and in the central plain of the Basin and exhibit varying degrees of degradation. The soils beneath the two shrub types comprised different amounts of igneous alluvium and sandy deposits. The creosotebush are usually located on the highly eroded, but predominantly locally sourced alluvium soils of the bajada. In comparison, the soils beneath mesquite are often composed of a larger percentage of

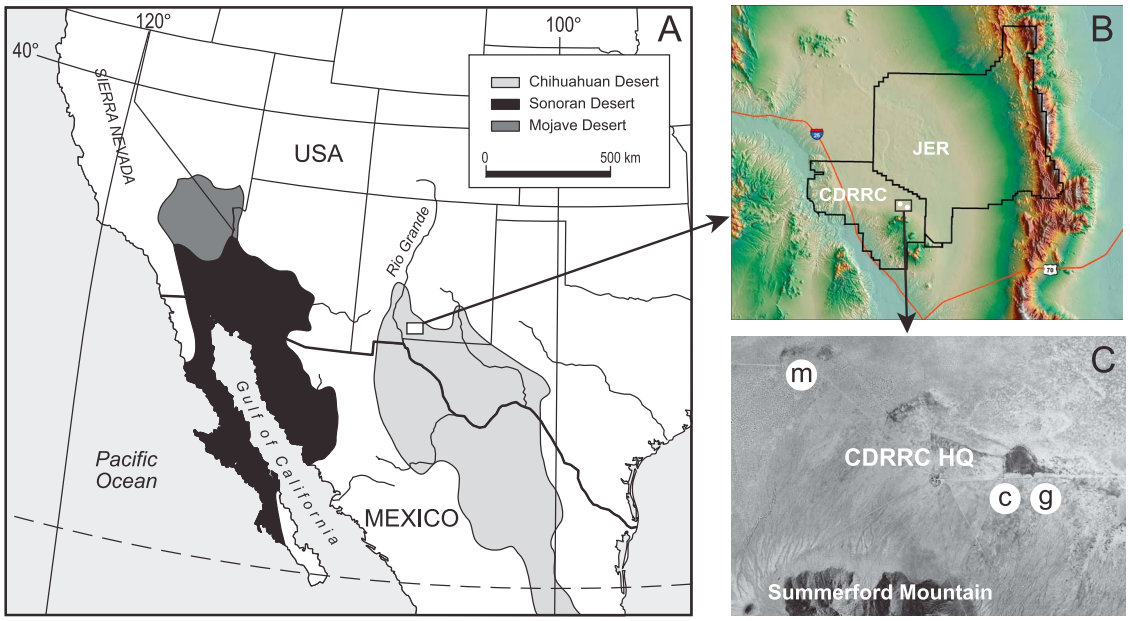

Figure 1. (a) Location of Jornada Long-Term Ecological Research (LTER) site within the Chihuahuan desert, New Mexico, USA. (b) The LTER includes the 78,000 ha Jornada Experimental Range (JER) and the 22,000 ha Chihuahuan Desert Rangeland Research Centre (CDRRC). (c) Location within the CDRRC in Jornada of the area of *Prosopis glandulosa* (honey mesquite), designated "m" in the photograph; the area of *Larrea tridentata* (creosotebush), designated "c"; and *Bouteloua eriopoda* (black grama grassland), designated "g." Modified from *Michaelides et al.* [2009].

aeolian-deposited sand-sized materials [*Gibbens et al.*, 2005; *Stein and Ludwig*, 1979] comprising a coating of clay and iron-oxide [*Monger et al.*, 2006]. Figure 1 shows the location of the different vegetation types within the study area.

3. Methods

3.1. Field Experiments

[9] Fifty-four small-scale rainfall-simulation experiments (1 m × 1.5 m) were undertaken in the Jornada Basin in order to characterize the runoff and erosion dynamics within three distinct vegetation communities. Of the 54 total experiments, a subset of 30 was analyzed for dissolved nutrient fluxes in the runoff and a further subset of 15 was analyzed for sediment-bound nutrient fluxes on the eroded sediment. Experiments were undertaken within each of the vegetation communities—the black grama grassland, and in the shrub and intershrub areas of creosotebush and mesquite. The intershrub areas were included in order to represent the microtopographical variations of the shrubland and to capture the variability in the plant characteristics within each vegetation type. Moreover, the intershrub areas are considered the predominant routes for runoff and eroded-sediment transport within the shrub communities [*Wainwright et al.*, 2000]. We focus on the plant-interplant scale because it is regarded as one of the fundamental scales of heterogeneity in these degrading dryland landscapes [*Wainwright et al.*, 2000]. Our experimental plots wholly encompass either individual plant canopies or bare interplant areas in order to capture the runoff and sediment flux characteristics determined by the vegetation type. In the grassland areas, our plots incorporate both plant and interplant areas as the grass canopy is significantly smaller than that of the shrubs.

[10] Each runoff plot was bounded on three sides by 15-cm-tall metal plates, approximately 5 cm of which was pushed into the soil, with a collection gutter dug into the fourth downslope end of the plot [*Bolton et al.*, 1991; *Parsons et al.*, 2003]. Rainfall simulation was used because: it overcomes the temporal and spatial variability in precipitation; it allows a controlled comparison of runoff and erosion dynamics between vegetation types; it allows a series of experiments to be undertaken under similar antecedent conditions and a reduction in the variability of external factors; and it facilitates the repetition of experiments. Small-scale plots were used to enable multiple experiments to be established within each vegetation type, to isolate the runoff/erosion dynamics and flux of nutrients from individual plant species, and because small plots are more cost-effective, practical and water-conservative than large rainfall-simulation plots. It should be recognized however that, despite their many advantages, small plot experiments do also have limitations: 1) they yield no information on time- and space-scale dependency in fluxes [e.g., *Brazier et al.*, 2007] and therefore cannot be reliably used to estimate annual fluxes; and 2) they provide no information on storm-pattern or rainfall rate effects on fluxes [e.g., *Parsons and Stone*, 2006].

[11] The experiments were conducted at a rainfall intensity of 125 mm h^{-1} ±13% for between 16 and 30 min. This rainfall rate and duration has an estimated return period of ~85 years in the Jornada Basin [*Wainwright*, 2006] but this is likely to be an underestimation due to the inefficiency of tipping-bucket rain gauges at high rainfall intensities and due to the lack of rainfall data in dryland environments [*Nicholson*, 2011]. Such a high intensity was used because it represents rainfall rates typical of the monsoonal rains in the area [*Nicholson*, 2011; *Wainwright*, 2006] and which have

been found to generate a disproportionate amount of the total runoff and erosion within drylands [*Howes and Abrahams*, 2003; *Martinez-Mena et al.*, 2001]. In addition, similar high intensities were used in previous rainfall-simulation studies in the same environments [e.g., *Parsons et al.*, 2003; *Schlesinger et al.*, 1999] and so were used again in this study to enable comparisons. Runoff and eroded sediment were collected in sterile polyethylene bottles via the gutter at the downslope edge of the plot. The sampling protocol followed that of *Schlesinger et al.* [1999] whereby collection of the first sample commenced at the point of runoff initiation and ceased once sufficient sample was available for analyses. The remaining samples were collected for 15 s every 1–4 min. The sampling intervals became longer during the latter half of the simulations as runoff reached equilibrium [*Schlesinger et al.*, 1999]. Following collection, the samples were filtered within 4 h to 0.45 μm using a polypropylene membrane filter in order to obtain a filtrate and a sediment fraction. The eroded-sediment samples were then air-dried and particle-size analysis was undertaken according to the Wentworth classification scheme. The samples were dry-sieved and a sub-sample of the <0.063 mm fraction was analyzed for the percentage of clay using a Malvern Mastersizer. Grain-size distributions (GSD) for sediment data were analyzed using GRADISTAT software [*Blott and Pye*, 2001] to obtain a characteristic grain size (D_{50}) by logarithmic method of moments. Intact surface soil samples from each plot were taken prior to the experiments in order to characterize soil surface stores of each nutrient and the soil properties (GSD, soil moisture, organic matter content).

3.2. Analytical Procedures

3.2.1. Nutrient Analyses of the Runoff Filtrate

[12] The runoff filtrate from each timestep in the experiments was analyzed for dissolved ammonium (NH_4^+), nitrite (NO_2^-), total oxidized nitrogen (TON), and phosphate (PO_4^{3-}) using a continuous segmented-flow Bran and Luebbe Autoanalyser (AA3). Dissolved nitrate (NO_3^-) was calculated by subtracting the dissolved NO_2^- from the TON. Total dissolved nitrogen (TDN) and total dissolved phosphorus (TDP) in the filtrate were analyzed using a persulphate digestion procedure, followed by detection on a Shimadzu UVmini1240 spectrophotometer for the presence of NO_3-N and PO_4-P. Potassium (K^+) concentrations were measured on a Perkin Elmer Optima 4300 DV ICP-OES (Inductively Coupled Plasma Optical Emission Spectrometer).

[13] Major cations and anions (Ca^{2+}, Mg^{2+}, Na^+, Cl^-, SO_4^{2-}, HCO_3^-) were measured to indicate weathering processes that might relate to N, P and K release, and to identify ion exchanges over the course of the rainfall simulations [*Lorrain and Souchez*, 1972]. Dissolved K+, Mg^{2+}, Na^+ and Ca^{2+} concentrations were measured on a Perkin Elmer Optima 4300 DV (Dual View) ICP-OES (Inductively Coupled Plasma Optical Emission Spectrometer). The accuracy of the ICP-OES in determining the major cations was assessed using an initial calibration verification (ICV) standard manufactured by CPI International, at a concentration of 100 mg l^{-1}. The concentrations of dissolved Cl^- and SO_4^{2-} were measured using a Dionex ICS90 Ion Chromatograph with an AS14A-5 μm analytical column and an AG14A guard column. HCO_3^- concentrations were determined by the charge balance between the positive and the negative ions [*Chadwick et al.*, 1994].

[14] The analytical accuracy associated with the solute data was calculated using reference standards applicable to each instrument, and are presented for each set of results. Method precision was calculated from either calibration standards that were treated as samples and analyzed intermittently in each run, or from at least three aliquots of a number of samples, which were analyzed within the same run or over several different runs. The detection limit of each method was determined by running a series of blanks. The equations used to determine analytical accuracy and precision are given in Appendix A.

3.2.2. Soil and Sediment Nutrient Extractions and Analyses

[15] Prior to the experiments, 10-cm soil samples were extracted from the surface adjacent to the plots and analyzed for soil properties and background nutrient concentrations. Species of N, P, K were extracted from the different size fractions of the eroded sediment in order to examine the relationship between the transported particle-size and nutrient transfers from the vegetation communities, and to reduce error margins associated with the small amounts of sediment used in the nutrient extraction processes.

[16] Soil and eroded-sediment samples were analyzed for the inorganic labile fractions of nitrogen (NO_3-N and NH_4-N) and TN, labile phosphorus (PO_4-P) and TP, and exchangeable K^+. Surface soil samples were also analyzed for Fe/Al-bound and apatite-bound P in order to compare the fractionation of P between vegetation types. NO_3-N and NH_4-N were extracted from the soils and sediment using a KCl solution, following a method by *Maynard and Kalra* [1993]. The resultant filtrate was tested for NO_3-N and NH_4-N on a Shimadzu UVmini1240 spectrophotometer and TN was analyzed using a Carlo Erba EA1108 Elemental Analyzer. P fractions were sequentially extracted from soil samples using a series of solutions adapted from procedures by *Hedley et al.* [1982] and *Mumford* [2003] (see Appendix B). P concentrations from the resultant filtrate were obtained using the phosphomolybdate method of *Murphy and Riley* [1962] on a Shimadzu UVmini 1240 spectrophotometer. The exchangeable K^+ fraction was extracted using 1 M ammonium acetate, following the first step of the Tessier scheme. The resultant filtrate was analyzed for K^+ on a Varian SpectraAA 220 FastSequential atomic absorption spectrophotometer (AAS) at 766.5 nm.

[17] Precision of the extraction techniques was established by analyzing three sub-samples of a number of different samples and different particle sizes for each nutrient species. Instrumental accuracy was determined using reference standards, and detection limits were established using blanks and the formula given in equation (A4) in Appendix A.

3.2.3. Rainwater Chemistry

[18] The water used in the rainfall-simulation experiments was obtained from nearby water tanks that consisted mainly of groundwater reserves. Natural rainwater was not available for use and de-ionized water would have flushed the ions from the soil [*Borselli et al.*, 2001]. Although concentrations of N and P species in the simulated rainfall were comparable with those found in natural rainfall, the major cation and anion concentrations were significantly higher than those in natural rainfall events. For example, the K^+ concentration in

Table 1. Mean and Standard Deviation of Nutrient Stores (G) in the Surface Soil Layer of the Experimental Plots (0.1 M Deep × 1 M × 1.5 M) According to Vegetation Type, Based on N = 9

Nutrient Species	Labile NH_4-N	Labile NO_3-N	Total N	Labile PO_4-P	Fe-bound PO_4-P	Apatite-bound PO_4-P	Total P	Exchangeable K^+
Vegetation type	Mean (g) ± s.d.							
Creosotebush shrub	0.8 ± 0.3	0.7 ± 0.1	63.3 ± 87.8	2.5 ± 0.8	2.2 ± 1.0	80.3 ± 11.8	95.6 ± 12.6	73.1 ± 28.3
Creosotebush intershrub	2.1 ± 0.1	1.3 ± 0.7	66.0 ± 66.3	3.2 ± 0.5	2.2 ± 0.3	85.3 ± 18.5	102.7 ± 18.9	89.2 ± 14.6
Grass	1.5 ± 1.1	1.3 ± 0.7	203.8 ± 163.8	4.0 ± 1.0	3.0 ± 1.1	121.1 ± 13.1	144.3 ± 14.1	160.0 ± 20.3
Mesquite shrub	2.4 ± 0.2	0.9 ± 0.6	20.4 ± 11.1	3.3 ± 1.3	3.8 ± 0.9	11.1 ± 4.6	25.4 ± 8.1	69.7 ± 15.5
Mesquite intershrub	1.3 ± 0.1	0.9 ± 0.6	48.9 ± 51.5	1.1 ± 0.6	3.9 ± 0.4	7.9 ± 1.6	22.0 ± 1.8	87.4 ± 52.7
ANOVA OUTCOME (p=)	0.073	0.651	0.346	0.023	0.090	<0.01	<0.01	0.017

the simulated rainfall water was two orders of magnitude greater than in the natural rainfall. Such high concentrations have implications for ion exchanges during the experiments. Desorption of NH_4^+ may have been facilitated by the high concentrations of Mg^{2+}, K^+ and Ca^{2+} in the experimental rainwater by providing competition for sorption sites. The source of water and its chemical composition is a limitation but provided the best available option for this field-based study considering the constraints of proximity, volume requirements and chemical composition.

4. Results

4.1. Soil-Nutrient Content

[19] In general, the apatite/calcite-bound P content of the soils was between one and two orders of magnitude greater than the labile and Fe-bound P content (Table 1). The apatite and calcite present in the Jornada soils locks up a substantial amount of P in the soil system, rendering it unavailable to vegetation until it can be released by dissolution [*Cross and Schlesinger*, 2001]. The Total N stores were at least five times larger than the inorganic labile NH_4-N and NO_3-N stores, indicating the significant contribution of the organic N fraction to the Total N present in the surface soils.

[20] The soil stores of labile P, apatite/calcite-bound P, Total P and exchangeable K^+ were significantly different according to vegetation type (Table 1), with the grassland typically containing the largest, and the mesquite intershrub plots the smallest stores of each of these nutrient fractions. Comparison of the shrub and intershrub soils showed significant differences only between stores of labile NH_4^+ (ANOVA, $p = 0.002$ and 0.012 for the mesquite and creosotebush respectively). The Total P content in the surface soils of the mesquite shrubland (shrub and intershrub plots) was significantly lower than the creosotebush shrubland and grassland (t-test, $p < 0.001$), illustrating the overriding sediment-source control on the nutrient content of the Summerford bajada soils. For example, the presence of aeolian-reworked sediments in addition to the quartz monzonite in the mesquite soils led to a four- to ninefold reduction in the apatite/calcite-bound P compared to the creosotebush and grassland soils.

[21] The vegetation influence on the surface-soil store of the three forms of N and the Fe-bound P was not found to be statistically significant (ANOVA, $p > 0.05$). The N species are not significantly sediment-derived, and were thus not statistically different according to vegetation type or to the source of the sediments. A notable store of labile and Total N forms was found in the surface soils, and this N could be a significant source for vegetation growth, particularly when dissolved N is limited.

4.2. Runoff and Erosion Characteristics

[22] Runoff yield was significantly lower in the mesquite shrubs than all the other vegetation types (Kruskal-Wallis (KW) test, $p < 0.01$ and Figure 2a) yet sediment yield exhibited the highest range. The grassland, creosotebush shrub and creosotebush intershrub plots produced similar runoff and sediment yields (Figures 2a and 2b) despite high variability in discharge and erosion rates within these

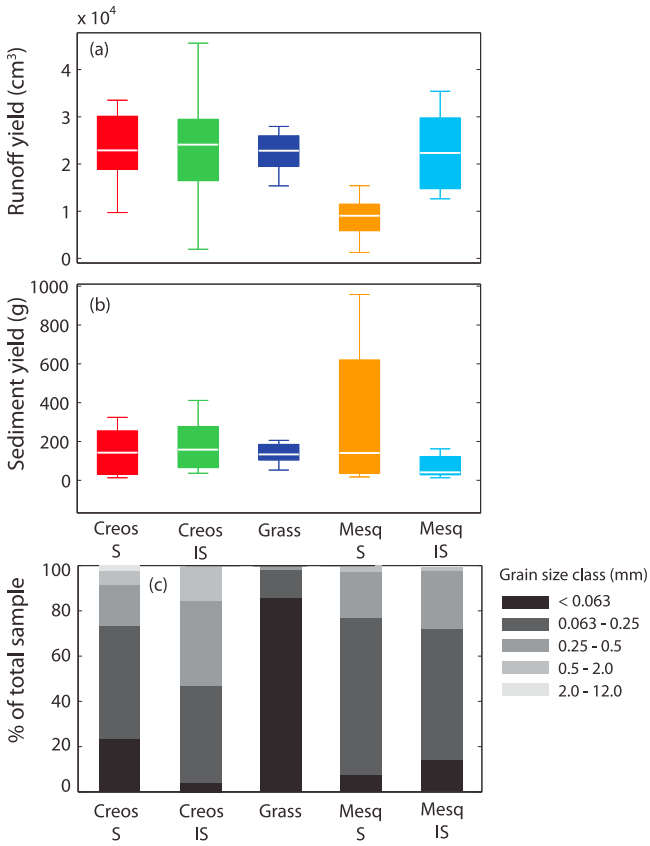

Figure 2. (a) Runoff yields (cm^3), (b) eroded sediment yields, and (c) grain-size distributions of the eroded sediment from the different vegetation types, where S = shrub and IS = intershrub. Yields are calculated as total mass exported from the 1.5 m^2 plots over 16 min of the simulation.

Table 2. Mean Volume-Weighted Dissolved Concentrations (Mg L^{-1}) for Each Nutrient According to Vegetation Type, With Means and Standard Deviations Based on N = 18

Nutrient Species	NH_4–N	NO_2–N	NO_3–N	PO_4–P	K
Vegetation type	Mean (mg l^{-1}) ± s.d.				
Creosotebush shrub	0.36 ±0.21	0.010 ±0.007	1.81 ±0.08	0.11 ±0.08	12.45 ±2.67
Creosotebush intershrub	0.08 ±0.06	0.005 ±0.002	1.72 ±0.17	0.03 ±0.01	8.41 ±1.35
Grass	0.14 ±0.07	0.017 ±0.009	1.99 ±0.33	0.07 ±0.03	13.46 ±1.83
Mesquite shrub	0.20 ±0.19	0.011 ±0.007	1.85 ±0.19	0.08 ±0.02	9.17 ±1.56
Mesquite intershrub	0.11 ±0.05	0.005 ±0.001	1.80 ±0.16	0.04 ±0.01	7.00 ±0.44

vegetation types [*Michaelides et al.*, 2009]. The most striking difference in the particle size composition of the eroded sediment (Figure 2c) is that the grassland plots produce the highest proportion (>80% by mass) of fine sediment (<0.063 mm) compared to all the other vegetation types. Based on 9 samples from 3 replica experiments in each vegetation type, the calculated D_{50} of the eroded sediment from the grassland was 0.18 mm compared to 0.48 mm for the creosotebush, 0.43 mm for the mesquite, 0.58 mm for the creosotebush intershrub and 0.37 mm for the mesquite intershrub.

[23] We have previously shown how vegetation type exerts first-order control on runoff and sediment dynamics at the plant scale, primarily through interactions between the plant-canopy characteristics, local mound gradient, crust cover and surface aggregate stability [*Michaelides et al.*, 2009]. Our findings show that the mesquite shrubs produce a significantly different response in terms of the relationship between runoff and sediment yield, compared to the other vegetation types. However, the grassland plots lose the highest percentage of fines, despite having similar runoff and sediment yields to the other vegetation types [*Michaelides et al.*, 2009].

4.3. Nutrient Concentrations and Fluxes in the Runoff

[24] Concentrations of N and P species in the runoff (Table 2) were not significantly correlated with the concentrations in the rainfall (regression, $p > 0.05$), and the concentrations in the rainfall were not found to be significantly different according to vegetation type (KW test, $p > 0.05$). Therefore, any differences in N and P concentrations can be directly attributed to vegetation type. Concentrations of K^+ in the runoff (Table 2) were found to be significantly related to those in the rainfall (regression, $p = 0.045$). However, K^+ concentrations in the rainfall were not significantly different according to vegetation type (KW test, $p = 0.93$). Therefore, differences in concentrations of K^+ produced in the runoff are assumed to reflect differences in K^+ concentrations in the soil.

[25] Instantaneous nutrient fluxes were calculated as the ratio of total nutrient yield in the runoff or bound to sediment (from the 1.5 m^2 plot area) to a fixed simulation time. We used 16 min as it was the minimum simulation time for all experiments. The dissolved nutrient fluxes according to vegetation type are presented in Figure 3. The highest fluxes of dissolved NH_4^+ were generated from the creosotebush shrubs (KW test, $p < 0.05$) while the highest fluxes of dissolved NO_2^- and K^+ were produced by the grassland (ANOVA, $p < 0.01$ and KW test, $p < 0.01$ respectively). Dissolved fluxes of NO_3^-, Total N, PO_4^{3-} and Total P were not found to vary significantly between vegetation types (KW test, $p > 0.05$). The mesquite shrubs produced consistently low fluxes of each dissolved nutrient species. Dissolved yields of NO_3-N and K+ were positively correlated to runoff yields (i.e., were transport limited), which further suggests that there was no significant limitation in the supply of $NO3^-$ and K^+ in any of the vegetation types. Conversely, NH_4-N, NO_2-N and PO_4-P were more strongly correlated to the N and P concentrations than the runoff yields (i.e., were supply limited) (Figure 4) suggesting that there is significant variation in these concentrations between vegetation types and that they control the flux.

[26] The soil C/N ratios (Table 3) highlight other differences between the vegetation communities. The high C/N ratio in the creosotebush soils suggests low presence of nitrifying bacteria [*Booth et al.*, 2005] and provides further explanation for the high NH_4-N fluxes from the creosotebush and the strong relationship to the NH_4^+ concentrations. In contrast, relatively high yields of NO_2-N and NO_3-N are seen for the grassland which has the lowest C/N ratio of all the vegetation types.

4.4. Sediment-Bound Nutrient Fluxes

[27] The grassland exhibited the highest sediment-bound fluxes of Total N (mainly consisting of organic N), labile PO_4^{3-}, Total P and exchangeable K^+ (Figures 5c–5f), and the mesquite shrubs produced the highest fluxes of NH_4^+ and NO_3^- (Figures 5a and 5b). The following sections breakdown these fluxes in terms of the grain-size-specific nutrient yields (total mass fluxed), the sediment-bound nutrient concentrations and the nutrient-enrichment ratios.

4.4.1. Grain-Size-Specific Sediment-Bound Nutrient Yields

[28] The contributions of each particle-size fraction to the overall sediment-bound yield of N, P and K species for each vegetation type were calculated (Figure 6). The sediment-bound nutrient yields were calculated as the sum of the sediment yield in each grain size fraction (<0.063 mm, 0.063–0.25 mm, 0.25–0.5 mm and 0.5–2.0 mm), multiplied by the nutrient concentration measured in that fraction. Yields were calculated for the first 16 min of each rainfall simulation for comparison between all experiments. Where there was insufficient sample available for analysis, and therefore concentration data are missing, calculated yields are incomplete and are presented in faded colors.

[29] The highest sediment-bound yields of Total N, P species and K are from the grassland plots (Figures 6c–6f), and of the NH_4-N and labile NO_3-N from the grassland and mesquite plots (Figures 6a and 6b). Sediment bound yields of all nutrients were higher from the vegetated areas than from the bare, intershrub areas. Figures 2 and 6 illustrate the importance of erosion dynamics for nutrient losses by affecting not only the total mass loss of sediment, but also the grain size characteristics of the eroded sediment. In the case of the grassland plots, eroded sediment yield was not significantly different from the creosotebush shrub or the intershrub areas, but the eroded sediment was significantly enriched in fine sediment (<0.063 mm) compared to all other vegetation types. The high yield of fines resulted in a significantly higher loss of most nutrient species from the grassland

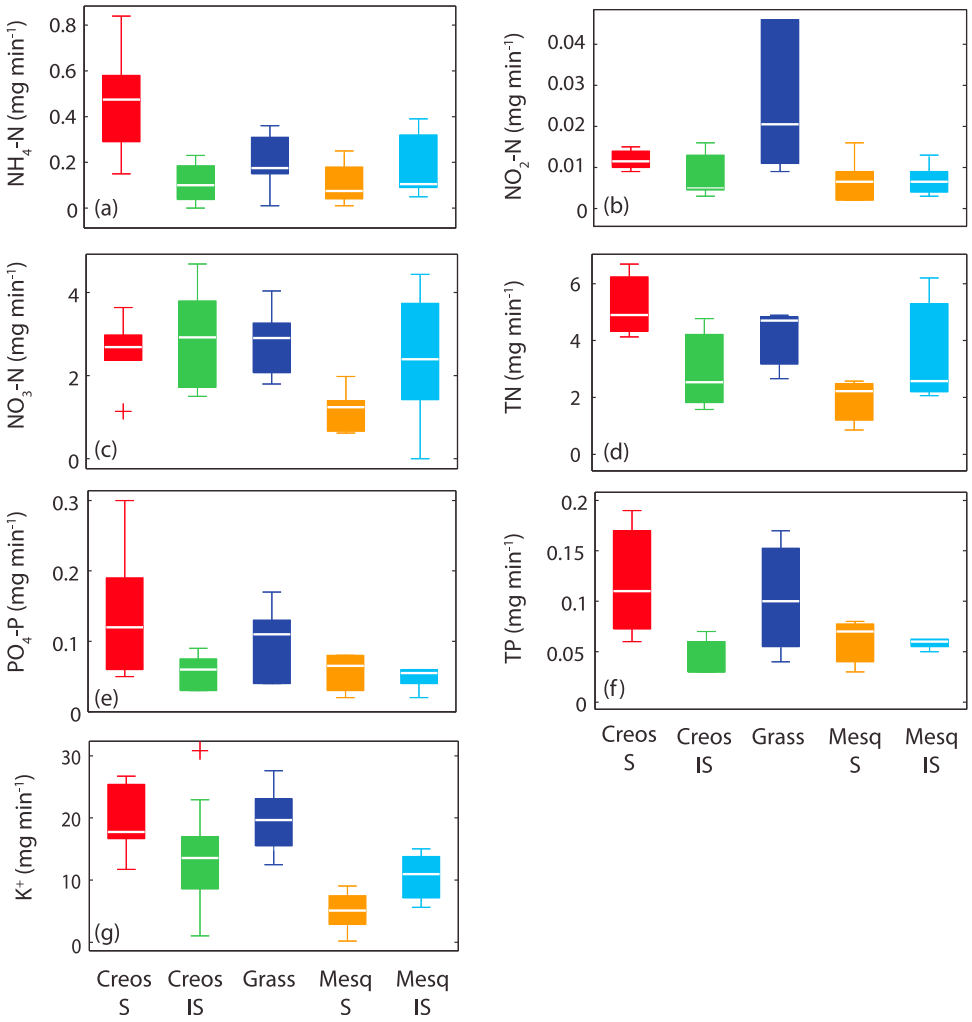

Figure 3. Dissolved nutrient fluxes (mg min^{-1}) according to vegetation type for: (a) ammonium, (b) nitrite, (c) nitrate, (d) total nitrogen, (e) phosphate, (f) total phosphorus and (g) potassium, where S = shrub and IS = intershrub.

than all the other vegetation types. On the other hand, the mesquite shrubs produced significantly higher eroded sediment yields than the other vegetation types, and although not significantly enriched in the finest sediment fraction, it did contain a high proportion of sediment in the 0.063–0.25 mm category. The combination of high sediment yields and enrichment in the second finest grain-size class resulted in the highest yields of labile NO_3-N and NH_4-N, as well as the second highest losses of most nutrients except labile PO_4-P and TP.

4.4.2. Sediment-Bound Nutrient Concentrations

[30] The highest concentration of each nutrient species was associated with the smallest sediment-size fraction (<0.063 mm). For example, the highest concentrations of labile PO_4^{3-} and labile NH_4^+ were measured on the <0.063 mm fraction in 93% and 80% of the samples respectively. This result is compatible with other observations in a range of environments [e.g., *Burkholder*, 1992; *Haygarth et al.*, 2006; *Hodson et al.*, 2004] and relates to the smallest size fraction having the highest surface area to which the nutrient can potentially adsorb, and containing a large proportion of clay minerals which provide the majority of sorption sites. As illustrated in Figure 6, the erosion of the finest grain-size class has a significant impact on nutrient fluxes from the different vegetation communities.

[31] The labile NH_4^+ and NO_3^- concentrations measured on the eroded sediments were not significantly different according to vegetation type (Table 4, ANOVA, $p = 0.77$ and 0.13 for NH_4^+, and NO_3^- respectively) reflecting similarities between the surface-soil N concentrations within the different vegetation communities (Table 1). The lack of significant variation in NO_3^- concentrations between vegetation types was thus consistent in both dissolved and sediment-bound forms, and differences in the fluxes are considered to be primarily controlled by differences in runoff and erosion.

[32] In contrast, the concentrations of labile PO_4^{3-} and Total N were significantly different according to vegetation type (ANOVA, $p < 0.01$ and KW test, $p < 0.05$ for PO_4^{3-} and Total N respectively). They were higher in the eroded sediments generated from the grassland plots than from the shrubs and

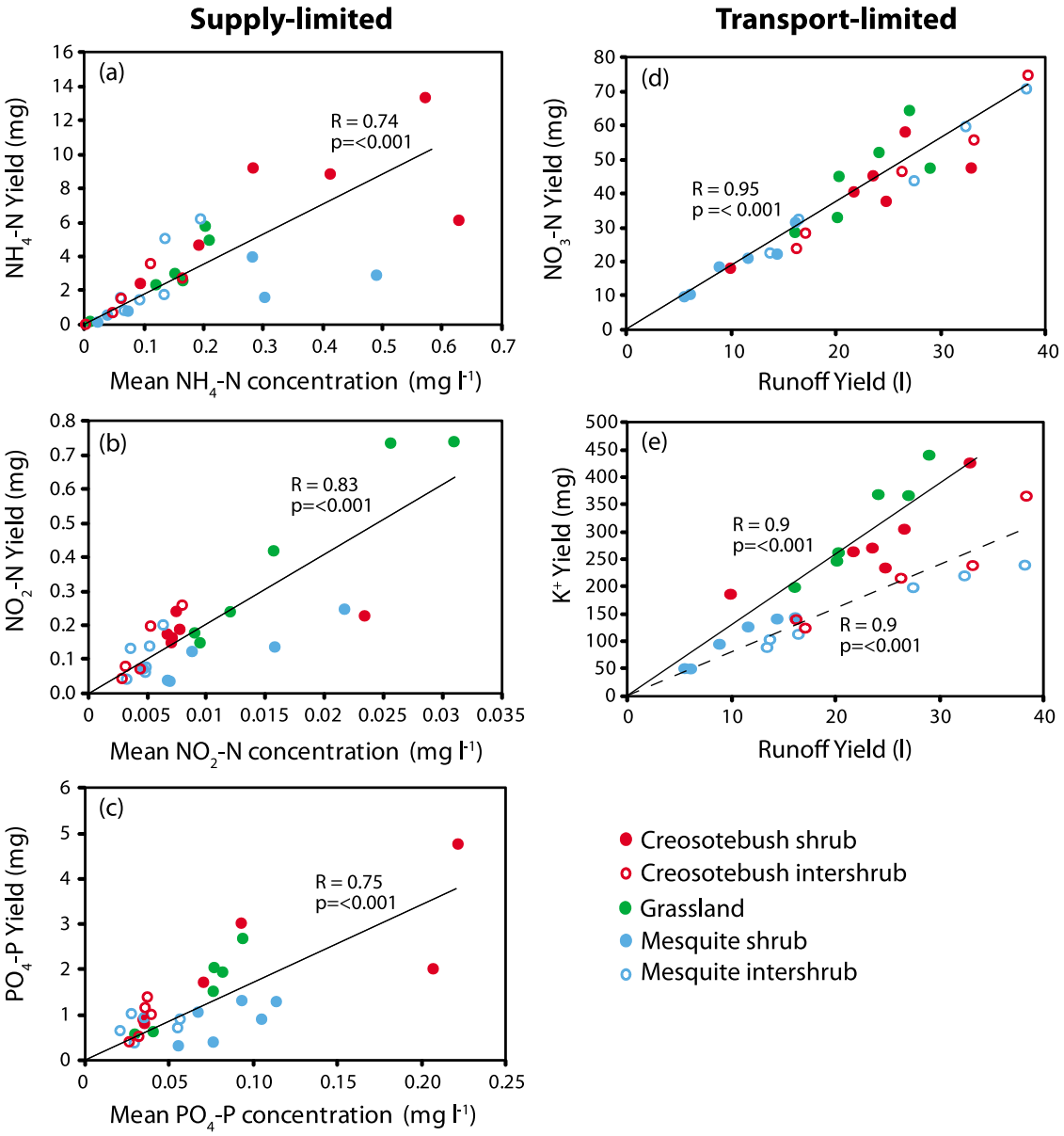

Figure 4. Relationships between nutrient yields and runoff yields or nutrient concentrations. (a), (b) and (c) are supply limited, and (d) and (e) are transport-limited. R is the correlation coefficient, and p is the significance at the 99% confidence level.

intershrub areas. The difference in concentrations of labile PO_4^{3-} on the eroded sediments reflects the larger store of labile PO_4^{3-} in the grassland (Table 1). In addition, labile PO_4^{3-} concentrations were significantly greater from the mesquite shrubs than their intershrub areas (2 sample t-test, $p < 0.01$). However, no significant differences were found in the Total N concentrations from the mesquite shrub compared to their intershrubs (2 sample t-test, $p = 0.801$) or in the labile PO_4^{3-} and Total N concentrations from the creosotebush shrub compared to their intershrub plots (2 sample t-test, $p = 0.41$ and 0.23 for the PO_4^{3-} and Total N respectively). Thus, any differences observed in the yields of these species are controlled by the erosion characteristics, either through variation in the sediment yield or the eroded grain-size characteristics.

[33] The concentrations of exchangeable K^+ were significantly different according to vegetation type (KW test, $p < 0.01$). The eroded sediments from the grassland contained the highest concentrations of exchangeable K^+ reflecting elevated concentrations of exchangeable K^+ found in the surface soils (Table 1). In addition, some of the highest dissolved K^+ concentrations were obtained from grassland

Table 3. C/N Ratios for Soils Beneath the Different Vegetation Types, With Means and Standard Deviations Based on N = 9

Vegetation Type	Mean C/N Ratio	s.d.	c.v. (%)
Creosotebush shrub	28	20	73
Creosotebush intershrub	51	48	95
Grass	15	8	56
Mesquite shrub	34	22	66
Mesquite intershrub	25	25	103

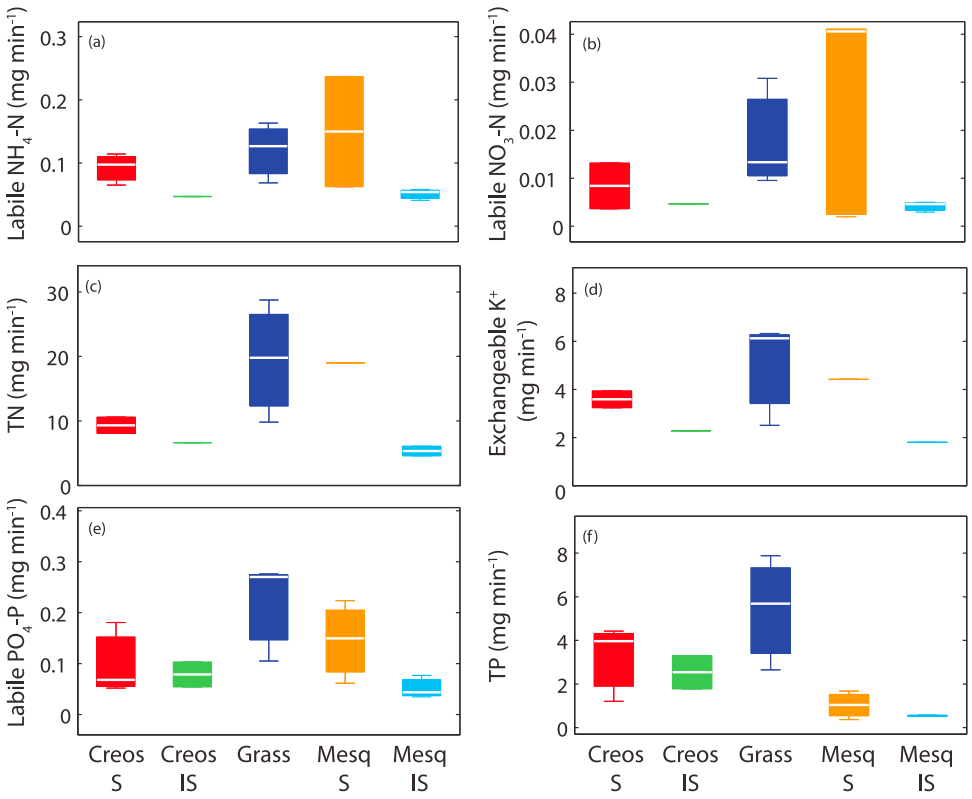

Figure 5. Sediment-bound nutrient fluxes (mg min^{-1}) according to vegetation type for: (a) labile ammonium, (b) labile nitrate, (c) total nitrogen, (d) labile phosphorus, (e) total phosphorus, and (f) potassium, where S = shrub and IS = intershrub.

plots. Thus, the K^+ concentrations from the grassland were high in both dissolved and sediment-bound forms relative to the shrubland sites.

[34] The concentrations of Total P were significantly different according to vegetation type (KW test, $p < 0.01$); the eroded sediments generated from the creosotebush shrub and intershrub and the grassland plots contained higher concentrations of Total P than the eroded-sediments from the mesquite shrub and intershrub areas (Table 4), again reflecting differences in surface-soil P content. The addition of aeolian-reworked Rio Grande sediments to the mesquite soils caused a reduction in the levels of Total P (particularly the apatite/calcite-bound fraction) and exchangeable K^+ compared to the soils of the creosotebush shrubland and the grassland.

4.4.3. Nutrient Enrichment Ratios

[35] The impact of preferential erosion on nutrient fluxes was further investigated by calculating nutrient enrichment ratios (ER = ratio of concentration of nutrients on the eroded sediment to the concentration of nutrients in the corresponding surface soils).

[36] The concentrations of labile NO_3^- attached to the eroded sediments were lower than in the surface soils in 65% of cases (Figure 7a). Due to its low negative valency, desorption of NO_3^- is facilitated making it less competitive for available sorption sites compared to other anions. Similarly, 70% of the eroded-sediment concentrations of exchangeable K^+ were significantly lower than the corresponding surface-soil concentrations (Figure 7c). Figure 8 suggests that during the rainfall simulations, K^+ was being desorbed into solution in exchange for Mg^{+2} in the majority of the experiments.

[37] In contrast, 79% of the eroded-sediment samples were at least three times enriched in Total N compared to the corresponding surface soils (Figure 7a). Most of the eroded sediment samples contained more than 100 times the Total N concentration of the surface soils. These high ratios suggest that a substantial amount of preferential erosion of sediment-bound organic N occurred during the erosion process. Total N concentrations in the eroded sediment did not significantly vary according to shrub presence or absence, echoing the lack of significant differences in surface-soil N content. Thus, despite vegetation being both a direct organic source and providing a preferred micro-climate for microbes, the results indicate that organic N is readily available within the Jornada environment.

[38] The direction of sorption kinetics for labile NH_4^+ and labile P concentrations was inconclusive from the data obtained in this study. The ERs for sediment-bound NH_4^+ were >1 in 50% of the samples investigated, equal to 1 in 34% of samples and <1 in the remaining 16% (Figure 7a). Similarly, the sediment-bound labile P ERs were >1 in 39% of samples, equal to 1 in 32% and <1 in 29% of samples (Figure 7b). Finally, in most eroded sediment samples (78%), Total P concentrations were either similar or slightly depleted relative to the surface-soils. The general similarity between the eroded-sediment and surface-soil might be expected for Total P given the dominant contribution (34%–84%) of the apatite-bound P fraction to the total sediment-bound P in the

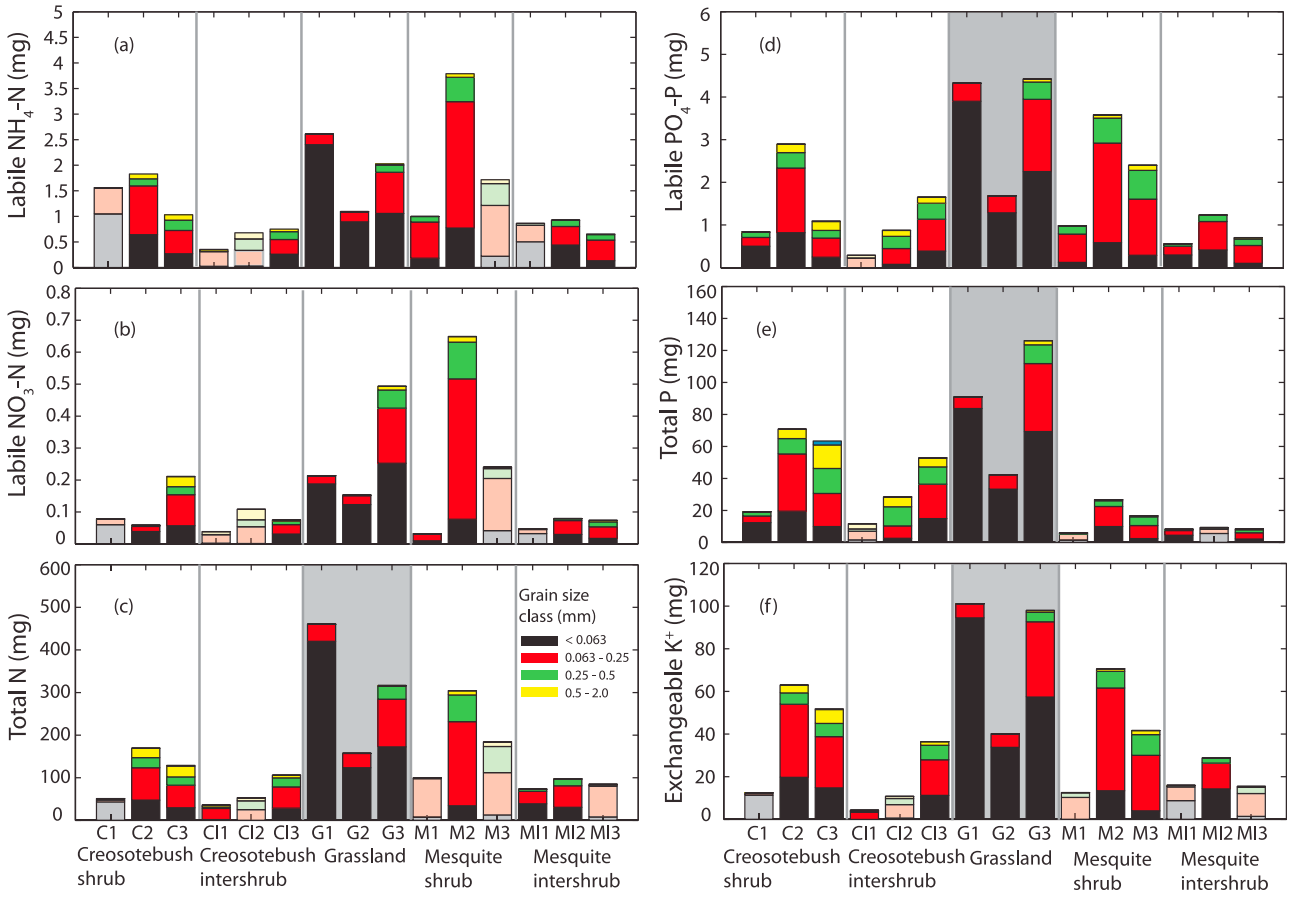

Figure 6. Sediment-bound yield of (a–c) N species, (d–e) P, and (f) K per particle-size fraction of the eroded sediment. All samples shown. The gray shading highlights the role of erosion of fine sediment from the grassland for nutrient export. Faded colors denote insufficient sediment sample for nutrient analysis and, therefore, incomplete yield.

surface soils. It is likely that the apatite-bound P fraction is not readily released into solution over the short timescale of a single rainfall event, as it is precipitated within the mineral complex of the soil.

5. Discussion

[39] The aim of this study was to investigate the linkages between the physical drivers of runoff and erosion and the nutrient fluxes they produce, in a degrading dryland landscape. Through a series of plant-scale rainfall simulation experiments we quantified the partitioning of N, P and K species between the dissolved phase in the runoff and the sediment-bound phase transported on eroded sediment, according to vegetation type. The results from our experiments show that the impacts of vegetation type on nutrient export are twofold: 1) biogeochemical processing and local nutrient loading, and 2) physical controls on runoff and erosion by the plant structure [see *Michaelides et al.*, 2009].

Table 4. Mean Sediment-Bound Nutrient Concentrations (Mg G^{-1}) Eroded From the Rainfall-Simulation Plots According to Vegetation Type (Adsorbed on the <0.063 Mm Grain Size Fraction), With Means and Standard Deviations Based on N = 9

Nutrient Species	Labile NH_4-N	Labile NO_3-N	TN	Labile PO_4-P	TP	Exchangeable K^+
Vegetation type			Mean (mg g^{-1}) ± s.d.			
Creosotebush shrub	0.03	0.003	2.05	0.03	0.70	0.77
	±0.02	±0.001	±0.58	±0.01	±0.14	±0.05
Creosotebush intershrub	0.02	0.002	1.69	0.02	0.75	0.56
	±0.01	±0.001	±0.38	±0.00	±0.07	±0.10
Grass	0.02	0.003	3.31	0.04	0.90	0.90
	±0.01	±0.001	±0.96	±0.01	±0.03	±0.12
Mesquite shrub	0.04	0.004	1.91	0.03	0.33	0.58
	±0.01	±0.003	±0.87	±0.01	±0.11	±0.19
Mesquite intershrub	0.03	0.002	2.02	0.02	0.29	0.69
	±0.01	±0.001	±0.81	±0.00	±0.06	±0.11

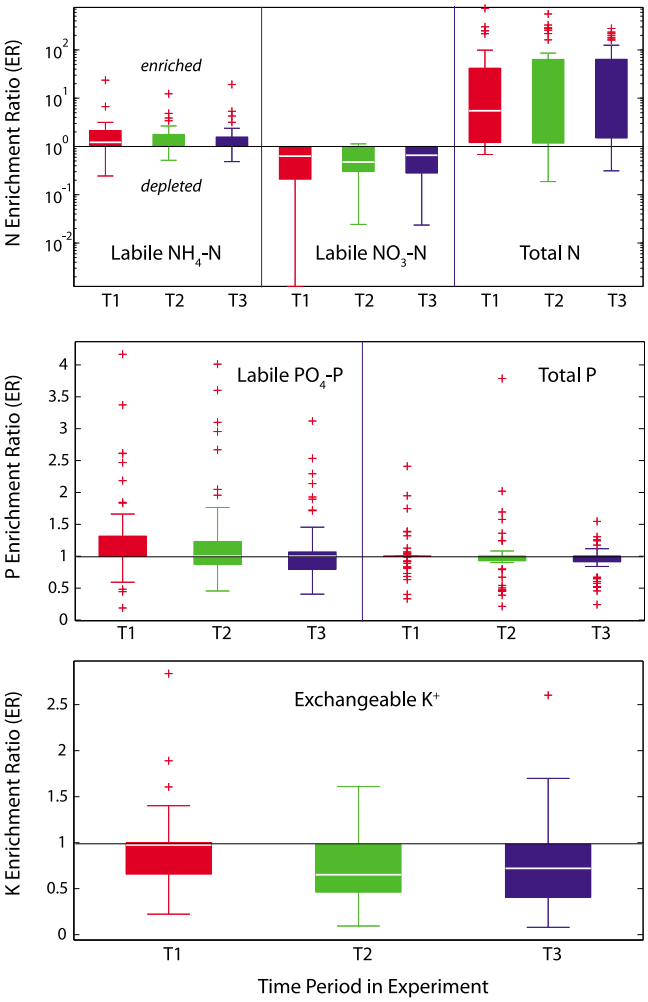

Figure 7. Enrichment ratios (ER = eroded-sediment nutrient concentrations/surface-soil nutrient concentrations) for fractions of (top) nitrogen, (middle) phosphorus, and (bottom) potassium. ER = 1 denotes equal concentrations in the eroded sediment and on the soil surface. The T1, T2, and T3 time slices represent the grouping of the 12 samples collected from each simulation into three time intervals containing equal numbers of samples, in order to attain sufficient sediment for analyzing according to particle size. T2 and T3 always spanned durations of 5 min and 12 min, respectively. T1 was variable between simulations and was dependent on the time to runoff initiation and the runoff rates at the start of the simulations.

The interaction between nutrient characteristics and runoff and erosion dynamics at the plant level, determine nutrient partitioning and fluxes out of the different vegetation communities with consequences for degradation processes.

[40] Although we did not specifically investigate plant biogeochemical processing, soil nutrient stores of labile P, apatite/calcite-bound P, Total P and exchangeable K^+ varied significantly according to vegetation type, with the largest nutrient stores found in the grassland, followed by the creosotebush shrub areas, and then by the mesquite shrub areas which had the smallest nutrient stores (Table 1). Furthermore, high C/N ratios in the shrub and intershrub plots suggest low nitrification rates [*Booth et al.*, 2005] in these areas in contrast to the low ratios in the grassland (Table 3), which affects the relative speciation and availability of N exported from the different vegetation types.

[41] Plant type and structure also exert a physical control on soil-surface characteristics and locally modulate the micropographic gradient, degree of crusting and soil grain-size distribution [*Michaelides et al.*, 2009; *Wainwright et al.*, 2000]. These soil surface variations affect local hydrology and result in different runoff and erosion responses. Our results highlight significant differences in the runoff and erosion dynamics between the vegetation types that manifest in three main ways: 1) variations in runoff fluxes, 2) differences in sediment fluxes, and 3) variations in the grain-size distribution of the eroded sediment.

[42] The linkage between the runoff and erosion dynamics and the local biogeochemical conditions, results in vegetation-specific variations in nutrient fluxes. For example, where a particular nutrient species is not supply limited in the surface soil, its flux out of the plot in dissolved form is determined by runoff flux rates. This situation occurs for NO_3^- and K^+ (Figure 3) and vegetation types with the highest runoff fluxes produce the largest yields of these nutrients and vice versa (i.e., the mesquite shrubs which produce the lowest runoff, also produce the smallest dissolved yields of NO_3^- and K^+). Where nutrients are supply limited in the surface soil and there is significant variation in this supply between vegetation types, dissolved nutrient fluxes are determined mainly by the nutrient concentrations. This case is exhibited in the cases of NH_4^+, NO_2^- and PO_4^{3-} (Figure 4), which have a stronger correlation to concentrations than to runoff yields. So, in the case of dissolved nutrient fluxes, we can consider the responses as being either transport-limited (nutrient is equally available everywhere so the flux is determined by the runoff) or supply limited (nutrient is not equally available everywhere so the flux is determined by local concentrations over runoff fluxes).

[43] Sediment-bound nutrient fluxes are determined by the erosion dynamics and the affinity for certain nutrient species to adsorb onto solid surfaces. The highest sediment-bound nutrient fluxes were produced by plots that either had the largest sediment yield (mesquite shrub) or the highest flux of fine sediment (<0.063 mm) regardless of the total sediment yield (grassland) (Figure 5). For TN, TP, labile PO_4^{3-}, and K^+ the grassland produced significantly higher fluxes compared to all other vegetation types due to the predominance of fine material eroded from these areas. For NO_3^- and NH_4^+, the highest sediment-bound fluxes were observed in the mesquite shrub as a result of the combination of the largest sediment yields and the relatively high concentrations of these nutrients in the mesquite soils (Table 1). Although grassland areas have finer textured soils compared to shrubland areas (see Table 2 in *Michaelides et al.* [2009]), initial soil texture alone does not account for the high proportion of fines eroded from the grassland plots (Figure 2c). Eroded sediment from the grassland plots is highly enriched in fines compared to all the other surface types as a result of the differing microtopography, surface properties and runoff characteristics between the grass and shrub areas [*Michaelides et al.*, 2009]. Therefore, although the grassland areas did not exhibit significantly higher runoff and eroded-sediment yields than any other vegetation type (Figure 2), the

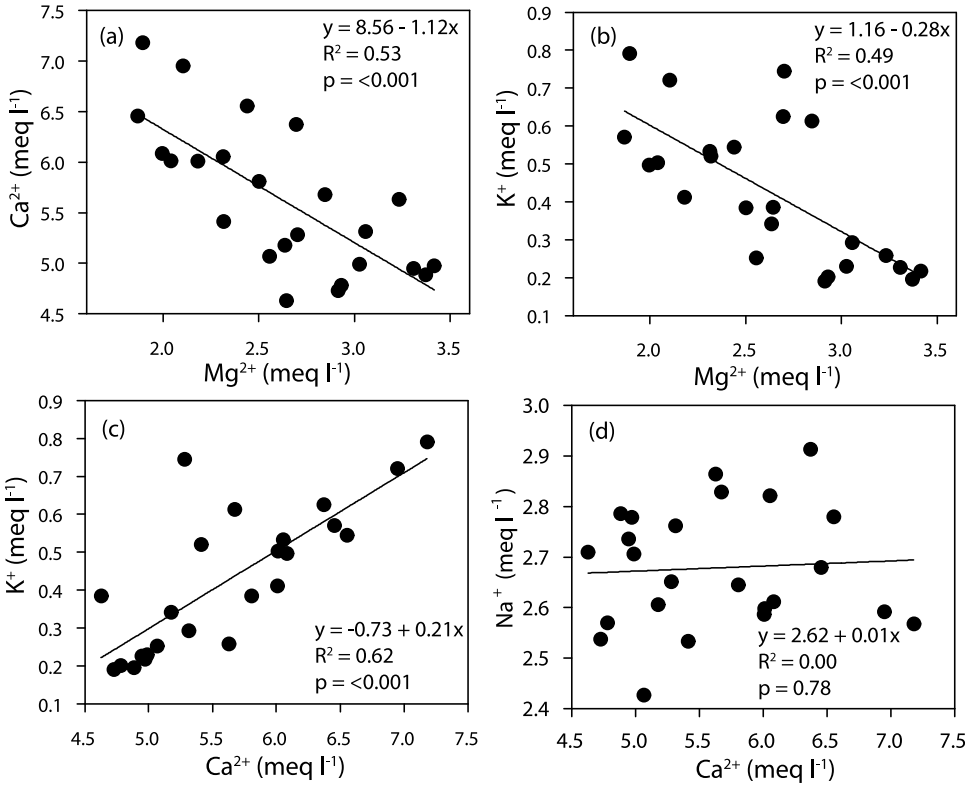

Figure 8. Relationships between mean cation concentrations in the simulated runoff: (a) Mg^{2+} and Ca^{2+}, (b) Mg^{2+} and K^{+}, (c) Ca^{2+} and K^{+}, and (d) Ca^{2+} and Na^{+}. Weighted cation concentrations in the runoff according to cation concentrations in the rainfall (C) were obtained by: $C = C_Q \times C_Q/C_R$, where C_Q is original cation concentration in the runoff and C_R is the cation concentration in the rainfall.

significant losses of fines led to the export of the highest sediment-bound yields in four out of six measured nutrient species. This result alone provides new evidence for existing hypotheses on land degradation processes in these dryland vegetation communities and supports previous work suggesting mechanisms by which grasslands are being supplanted by the shrubs [e.g., *Aguiar and Sala*, 1999; *Parsons et al.*, 2003; *Schlesinger et al.*, 1990; *Wainwright et al.*, 2002]. Although we did not explicitly consider inter-vegetation fluxes at the large scale, our findings suggest that if grassland areas are found upslope of the shrub areas within degrading landscapes, and are consistently exporting fine sediment enriched in bio-essential nutrients, shrub communities will likely benefit by accumulating these resources under their canopy and increasing their spatial distribution over the grasses [see also *Mueller et al.*, 2007]. In this grass-shrub transition the loss of nutrients results in the system moving to a lower resource state. Indeed, the importance of grain-size distributions of eroded sediment for runoff-driven sediment-bound nutrient fluxes has thus far not been demonstrated in these degrading dryland environments.

[44] Figure 9 summarizes the percentage input and output of all nutrient species in the dissolved and sediment-bound form, and Figure 10 illustrates the importance of sediment-bound nutrient fluxes in the Jornada landscape averaged across all vegetation types. The vast majority of exported ON and non-labile forms of P (>70% of the total exported) were sediment bound. Along with water, N has been defined as the most limiting nutrient for vegetation growth in

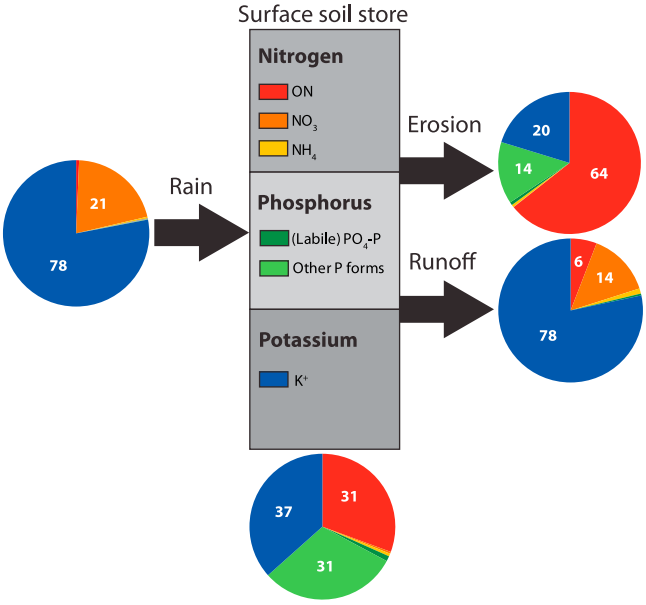

Figure 9. Summary of the inputs and outputs of dissolved and sediment-bound nutrient exports based on the rainfall-simulation experiments. Values are given as a percentage of the total input or output in the particular form (i.e., dissolved or sediment-bound) averaged across all vegetation types.

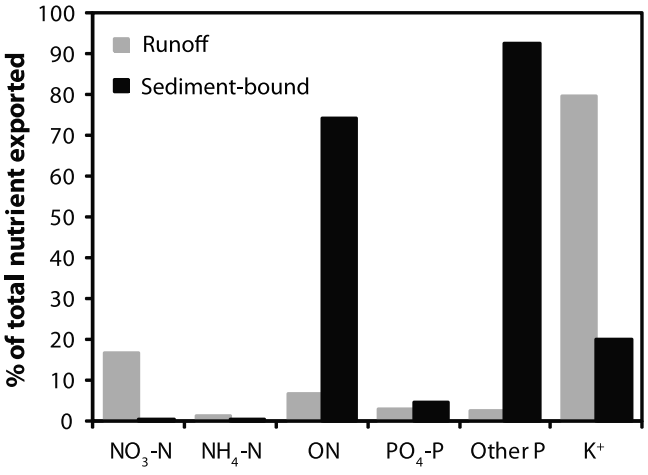

Figure 10. Comparison between dissolved and sediment-bound exports of all nutrients. Individual nutrient outputs are expressed as a percentage of the total mass of nutrient (dissolved + sediment-bound) exported from a plot. Results are averaged over all vegetation types (N = 15).

drylands [*Fisher et al.*, 1988; *Hooper and Johnson*, 1999]. Particular emphasis has been placed on the rapid flux of the dissolved inorganic N species as a key factor in land-degradation [*Schlesinger et al.*, 1999; *Schlesinger et al.*, 2000]. However, our results suggest that N is predominantly transported in the organic form and bound to eroded sediment rather than dissolved in runoff. Through mineralization, organic N is a potential source of bioavailable, inorganic N species and so its relocation has significant implications for vegetation competition. Dissolved fluxes of N consisted mainly of NO_3^-. Similarly, P was found to be predominantly exported adsorbed to eroded sediment and the largest proportion was in the non-labile form. The sediment-bound and dissolved fluxes of labile PO_4^{3-} were of similar magnitude, and typically lower than dissolved fluxes of inorganic N. The affinity of PO_4^{3-} to sediment has been cited as the reason for lower concentrations of dissolved P relative to N in runoff [*Schlesinger et al.*, 1999]. However, our results show similar fluxes of dissolved and sediment-bound PO_4^{3-} and equally high fluxes of sediment-bound N and P (Figure 10) which dominate the overall export of these nutrients. These findings corroborate results obtained at the larger scale (10 × 30 m plots) on plots with similar vegetation types at the Sevilleta LTER site in New Mexico [*Turnbull et al.*, 2011].

[45] Comparison of sediment-bound and dissolved fluxes of K^+ must be interpreted with caution because the concentrations of K^+ and the other major cations in the simulated rainfall were orders of magnitude higher than have been found in natural rainfall. Despite the large surface-soil store, K^+ losses were primarily in the dissolved form. Some of this loss resulted from desorption of the K^+ from sediment to solution, encouraged by the abundance of competitive cations in the runoff (particularly Mg^{2+} ions). Although the relative abundance of Mg^{2+}, Ca^{2+} and Na^+ relative to K^+ tends to be higher in natural rainfall than in the simulated rainfall, implying that cation exchanges and K^+ desorption would also have occurred during a natural rainfall event, scaling between real and artificial rainfall compositions is not straightforward, particularly as other cations and anions will also vary in their abundance between the two. Overall, K^+ is perhaps less likely to impose limitations on vegetation productivity in Jornada than either N or P, with such a large store of exchangeable K^+ present in the surface soils, and desorption of the exchangeable K^+ making it rapidly available to vegetation in the dissolved form during rainfall events.

[46] Our small-scale experiments have produced new insights into plant-scale controls on nutrient exports and their partitioning into dissolved and sediment-bound forms. Understanding plant-level controls on runoff and erosion dynamics and the impacts for nutrient fluxes is important for determining the relative importance of rainfall-driven resource redistribution between vegetation communities as a key process in dryland land degradation. Although the importance of sediment-bound N and P transfers within this dryland landscape have been found in previous studies [e.g., *Turnbull et al.*, 2011], the detailed dynamics of runoff and erosion that drive differences in nutrient fluxes from different vegetation types have thus far not been demonstrated. If plant-level runoff and erosion dynamics and the nutrient exports they drive can be assumed to be representative of the wider vegetation community, then our findings are commensurate with existing theories on land degradation processes. In particular, we have demonstrated the importance of grain-size distributions of the eroded sediment as a major driver of nutrient export from the grassland over and above total sediment yield, which is potentially distributed to, and used by, the shrub communities, promoting the process of land degradation.

6. Conclusion

[47] Land degradation in drylands has been attributed to a combination of factors, particularly to the linkages between vegetation changes, water and sediment redistribution and nutrient fluxes. A growing body of research into land degradation-dynamics is showing that bio-essential nutrients are being transported from the degrading to invading vegetation communities by wind and water, resulting in ongoing positive feedbacks that perpetuate degradation. Studies have also shown that runoff-driven erosion events that occur during the infrequent but often extreme rainfall events characteristics of many dryland environments are able to redistribute sediment [e.g., *Turnbull et al.*, 2011; *Wainwright et al.*, 2002] with implications for sediment-bound nutrient relocation. However, despite the well-documented significance of rainfall-driven erosion events as drivers of landscape change in these environments, their impact on sediment-bound nutrient fluxes remains poorly resolved. In this paper we address this gap through a series of rainfall simulation experiments designed to explore plant-level dynamics of runoff- and erosion-driven nutrient fluxes of N, P and K species. We focus particularly on the partitioning of nutrients dissolved in the runoff and bound to eroded sediments according to grain-size fraction, and we explore relationships between the physical drivers and the nutrient fluxes they produce.

[48] Our results highlight several key nutrient dynamics that arise due to linkages between physical and biogeochemical processes: 1) the magnitude of the export of nutrient bound to sediment is determined by the grain-size distribution of the eroded sediment and the total sediment yield; and 2) the partitioning of nutrient in dissolved and sediment-bound form is determined by the availability and

Table B1. Sequential Extraction Methodology, Adapted From *Hedley et al.* [1982], *Lajtha and Schlesinger* [1988], *Ruttenberg* [1992], and *Mumford* [2003]

Fraction of Phosphorus	Extraction Procedure	Procedure Details	Adjustment to pH 7 Prior to Colorimeter Analysis[a]
Loosely sorbed or labile phosphorus	$MgCl_2$ extraction	12 ml $MgCl_2$ (16 h) 12 ml H_2O (2 h) 12 ml H_2O (2 h)	None required
Iron- and aluminum-bound phosphorus	NaOH extraction	12 ml NaOH (16 h) 12 ml NaOH (2 h) 12 ml H_2O (2 h)	HCl solution (2 M and 1 M)
Apatite- and calcite-bound phosphorus	HCl extraction	12 ml HCl (16 h) 12 ml HCl (2 h) 12 ml H_2O (2 h)	NaOH solution (4 M and 1 M)
Residual phosphorus (non-reactive phosphorus)	$K_2S_2O_8$ digestion	15 ml $K_2S_2O_8$ plus 0.75 ml 4 M H_2SO_4 into an autoclave (10 min at 121°C, 15 PSI)	NaOH solution (6 M, 4 M and 1 M)

[a]Volume of solutions added to standards and samples for pH adjustment were recorded and results adjusted accordingly. The same overall volume of solution was added to each standard for pH adjustment to attain a usable calibration curve.

concentration of different nutrient species in the soil nutrient store or rainfall. We found that these processes varied according to vegetation type and resulted in stark differences between the degrading and invading plant species. Specifically, we observed that the grassland areas consistently exported the highest yields of sediment-bound N, P and K despite producing similar erosion rates to shrub and inter-shrub areas. This was due to the significantly higher proportion of fine sediments (<0.063 mm) eroded from the grassland than from any other vegetation type. Dissolved nutrient yields on the other hand, were a function of either runoff yields (if nutrients were not supply limited) or local concentrations in the runoff (if there was significant variation in local nutrient supply). Our previous research quantified the relationships between plant type and runoff and erosion dynamics [*Michaelides et al.*, 2009] and demonstrated a strong control of plant structure on the quantity and quality of eroded sediment fluxed from different vegetation types. In this paper we further link these plant-level runoff and erosion dynamics to nutrient transport, and our results overall demonstrate the importance of sediment-bound nutrient fluxes, particularly for the export of organic nitrogen and non-labile forms of phosphorus. Plant type was also found to exert a significant control on the rainfall-driven transport of sediment at small spatial scales [*Field et al.*, 2012].

[49] Our findings reinforce existing theories on land degradation in the Jornada landscape by providing direct support to the underlying assumptions that grassland areas lose nutrients at the expense of the shrubs and that rainfall-driven erosion is a significant contributor of vital nutrients to the islands of fertility.

Appendix A: Equations Used in the Determination of Analytical Accuracy and Precision

$$\text{Analytical accuracy (\% recovery)} = ((C_m - C_b)/C_a)/100 \quad \text{(A1)}$$

$$\text{Individual sample precision (\%)} = (\sigma/\bar{X}) \times 100 \quad \text{(A2)}$$

$$\text{Mean overall precision (\%)} = (\sum\sigma_a/\sum\bar{X}_a) \times 100 \quad \text{(A3)}$$

$$\text{Detection limit} = \bar{X}_b + (3 \times \sigma_b) \quad \text{(A4)}$$

where C_m = measured concentration of reference standard, C_b = mean concentration of blanks, C_a = actual concentration of reference standard, σ_a = standard deviation of the aliquots, $\bar{X}_a$ = mean of the aliquots, σ_b = standard deviation of the blanks, and $\bar{X}_b$ = mean of the blanks.

Appendix B: Sequential Extraction Methodology

[50] Table B1 shows the sequential extraction methodology used to obtain fractions of P in the eroded sediment and surface soil samples analyzed for this study.

[51] **Acknowledgments.** This research was funded by a NERC PhD studentship to DL. We thank the Jornada LTER program (NSF grant DEB 0080412) and New Mexico State University for their support during this research and for granting access to the field site. Paul Fletcher assisted with field work and Jenny Mills assisted with analytical procedures. We thank Richard Pancost (School of Chemistry, Bristol) and Ed Hornibrook (Department of Earth Sciences, Bristol) for granting access to analytical facilities. Barbara Nolen from LTER/NMSU kindly provided Figure 1c. We thank two anonymous reviewers for helpful comments on the original manuscript.

References

Aguiar, M. R., and O. E. Sala (1999), Patch structure, dynamics and implications for the functioning of arid ecosystems, *Trends Ecol. Evol.*, *14*(7), 273–277, doi:10.1016/S0169-5347(99)01612-2.

Blott, S. J., and K. Pye (2001), Gradistat: A grain size distribution and statistics package for the analysis of unconsolidated grains, *Earth Surf. Processes Landforms*, *26*, 1237–1248, doi:10.1002/esp.261.

Bolton, S. M., T. J. Ward, and R. A. Cole (1991), Sediment-related transport of nutrients from southwestern watersheds, *J. Irrig. Drain. Eng.*, *117*, 736–747, doi:10.1061/(ASCE)0733-9437(1991)117:5(736).

Booth, M. S., J. M. Stark, and E. Rastetter (2005), Controls on nitrogen cycling in terrestrial ecosystems: A synthetic analysis of literature data, *Ecol. Monogr.*, *75*(2), 139–157, doi:10.1890/04-0988.

Borselli, L., D. Torri, J. Poesen, and P. S. Sanchis (2001), Effects of water quality on infiltration, runoff and interrill erosion processes during simulated rainfall, *Earth Surf. Processes Landforms*, *26*(3), 329–342, doi:10.1002/1096-9837(200103)26:3<329::AID-ESP177>3.0.CO;2-Y.

Brazier, R. E., A. J. Parsons, J. Wainwright, D. M. Powell, and W. H. Schlesinger (2007), Upscaling understanding of nitrogen dynamics associated with overland flow in a semi-arid environment, *Biogeochemistry*, *82*(3), 265–278, doi:10.1007/s10533-007-9070-x.

Breshears, D. D., J. J. Whicker, M. P. Johansen, and J. E. Pinder (2003), Wind and water erosion and transport in semi-arid shrubland, grassland and forest ecosystems: Quantifying dominance of horizontal wind-driven transport, *Earth Surf. Processes Landforms*, *28*(11), 1189–1209, doi:10.1002/esp.1034.

Buffington, L. C., and C. H. Herbel (1965), Vegetational Changes on a Semidesert Grassland Range, *Ecol. Monogr.*, *35*, 139–164, doi:10.2307/1948415.

Burkholder, J. M. (1992), Phytoplankton and episodic suspended sediment loading: Phosphate partitioning and mechanisms for survival, *Limnol. Oceanogr.*, *37*(5), 974–988, doi:10.4319/lo.1992.37.5.0974.

Chadwick, O. A., E. F. Kelly, D. M. Merritts, and R. G. Amundson (1994), Carbon dioxide consumption during soil development, *Biogeochemistry*, *24*, 115–127, doi:10.1007/BF00003268.

Charley, J. L., and N. E. West (1975), Plant-induced soil chemical patterns in some shrub-dominated semi-desert ecosystems of Utah, *J. Ecol.*, *63*(3), 945–963, doi:10.2307/2258613.

Cross, A. F., and W. H. Schlesinger (1999), Plant regulation of soil nutrient distribution in the northern Chihuahuan Desert, *Plant Ecol.*, *145*(1), 11–25, doi:10.1023/A:1009865020145.

Cross, A. F., and W. H. Schlesinger (2001), Biological and geochemical controls on phosphorus fractions in semiarid soils, *Biogeochemistry*, *52*(2), 155–172, doi:10.1023/A:1006437504494.

Field, J. P., D. D. Breshears, J. J. Whicker, and C. B. Zou (2012), Sediment capture by vegetation patches: Implications for desertification and increased resource redistribution, *J. Geophys. Res.*, *117*(G1), G01033, doi:10.1029/2011JG001663.

Fierer, N. G., and E. J. Gabet (2002), Carbon and nitrogen losses by surface runoff following changes in vegetation, *J. Environ. Qual.*, *31*, 1207–1213, doi:10.2134/jeq2002.1207.

Fisher, F. M., J. C. Zak, G. L. Cunningham, and W. G. Whitford (1988), Water and nitrogen effects on growth and allocation patterns of creosotebusg in the northern Chihuahuan desert, *J. Range Manage.*, *41*(5), 387–391, doi:10.2307/3899572.

Gabet, E. J., N. Fierer, and O. A. Chadwick (2005), Prediction of sediment-bound nutrient delivery from semi-arid California watersheds, *J. Geophys. Res.*, *110*(G2), G02001, doi:10.1029/2005JG000032.

Gibbens, R. P., R. P. McNeely, K. M. Havstad, R. F. Beck, and B. Nolen (2005), Vegetation changes in the Jornada Basin from 1858 to 1998, *J. Arid Environ.*, *61*(4), 651–668, doi:10.1016/j.jaridenv.2004.10.001.

Gile, L. H., R. P. Gibbens, and J. M. Lenz (1997), The near-ubiquitous pedogenic world of mesquite roots in an arid basin floor, *J. Arid Environ.*, *35*, 39–58, doi:10.1006/jare.1996.0157.

Haygarth, P. M., et al. (2006), Processes affecting transfer of sediment and colloids, with associated phosphorus, from intensively farmed grasslands: An overview of key issues, *Hydrol. Processes*, *20*(20), 4407–4413, doi:10.1002/hyp.6598.

Hedley, M. J., J. W. B. Stewart, and B. S. Chauhan (1982), Changes in inorganic and organic soil-phosphorus fractions induced by cultivation practices and by laboratory incubations, *Soil Sci. Soc. Am. J.*, *46*(5), 970–976, doi:10.2136/sssaj1982.03615995004600050017x.

Hodson, A., P. Murnford, and D. Lister (2004), Suspended sediment and phosphorus in proglacial rivers: Bioavailability and potential impacts upon the P status of ice-marginal receiving waters, *Hydrol. Processes*, *18*(13), 2409–2422, doi:10.1002/hyp.1471.

Hooper, D. U., and L. Johnson (1999), Nitrogen limitation in dryland ecosystems: Responses to geographical and temporal variation in precipitation, *Biogeochemistry*, *46*(1–3), 247–293, doi:10.1007/BF01007582.

Howes, D. A., and A. D. Abrahams (2003), Modeling runoff and runon in a desert shrubland ecosystem, Jornada Basin, New Mexico, *Geomorphology*, *53*, 45–73, doi:10.1016/S0169-555X(02)00347-1.

Kraimer, R. A., H. C. Monger, and R. L. Steiner (2005), Mineralogical distinctions of carbonates in desert soils, *Soil Sci. Soc. Am. J.*, *69*, 1773–1781, doi:10.2136/sssaj2004.0275.

Li, J., G. S. Okin, L. Alvarez, and H. Epstein (2007), Quantitative effects of vegetation cover on wind erosion and soil nutrient loss in a desert grassland of southern New Mexico, USA, *Biogeochemistry*, *85*(3), 317–332, doi:10.1007/s10533-007-9142-y.

Li, J., G. S. Okin, L. Alvarez, and H. Epstein (2008), Effects of wind erosion on the spatial heterogeneity of soil nutrients in two desert grassland communities, *Biogeochemistry*, *88*(1), 73–88, doi:10.1007/s10533-008-9195-6.

Lorrain, R. D., and R. A. Souchez (1972), Sorption as a factor in the transport of major cations by meltwaters from an Alpine glacier, *Quat. Res.*, *2*, 253–256, doi:10.1016/0033-5894(72)90043-9.

Martinez-Mena, M., V. Castillo, and J. Albaladejo (2001), Hydrological and erosional response to natural rainfall in a semi-arid area of south-east Spain, *Hydrol. Processes*, *15*(4), 557–571, doi:10.1002/hyp.146.

Maynard, D. G., and Y. P. Kalra (1993), Nitrate and exchangeable ammonium nitrogen, in *Soil Sampling and Methods of Analysis*, edited by M. R. Carter, pp. 25–38, Lewis, London.

Meybeck, M. (1982), Carbon, nitrogen, and phosphorus transport by world rivers, *Am. J. Sci.*, *282*, 401–450, doi:10.2475/ajs.282.4.401.

Michaelides, K., D. Lister, J. Wainwright, and A. J. Parsons (2009), Vegetation controls on small-scale runoff and erosion dynamics in a degrading dryland environment, *Hydrol. Processes*, *23*(11), 1617–1630, doi:10.1002/hyp.7293.

Monger, H. C. (2006), Soil development in the Jornada Basin, in *Structure and Function of a Chihuahuan Desert Ecosystem: The Jornada Basin Long-Term Ecological Research Site*, edited by K. Havstad et al., pp. 81–106, Oxford Univ. Press, Oxford, U. K.

Monger, H. C., G. H. Mack, B. A. Nolen, and L. H. Gile (2006), Regional setting of the Jornada Basin LTER, in *Structure and Function of a Chihuahuan Desert Ecosystem: The Jornada Basin Long-Term Ecological Research Site*, edited by K. Havstad et al., pp. 11–35, Oxford Univ. Press, Oxford.

Mueller, E. N., J. Wainwright, and A. J. Parsons (2007), The stability of vegetation boundaries and the propagation of desertification in the American Southwest: A modelling approach, *Ecol. Modell.*, *208*(2–4), 91–101, doi:10.1016/j.ecolmodel.2007.04.010.

Mumford, P. N. (2003), *Nutrient Budgets and Transport Dynamics in a High Arctic Glacier Basin, Svalbard*, Univ. of Sheffield, Sheffield.

Murphy, J., and J. P. Riley (1962), A modified single solution method for determination of phosphate in natural waters, *Anal. Chim. Acta*, *27*(1), 31–36, doi:10.1016/S0003-2670(00)88444-5.

Newman, E. I. (1995), Phosphorus inputs to terrestrial ecosystems, *J. Ecol.*, *83*(4), 713–726, doi:10.2307/2261638.

Nicholson, S. E. (2011), *Dryland Climatology*, Cambridge Univ. Press, Cambridge, U. K., doi:10.1017/CBO9780511973840.

Okin, G. S., P. D'Odorico, and S. R. Archer (2009), Impact of feedbacks on Chihuahuan desert grasslands: Transience and metastability, *J. Geophys. Res.*, *114*, G01004, doi:10.1029/2008JG000833.

Parsons, A. J., and P. M. Stone (2006), Effects of intra-storm variations in rainfall intensity on interrill runoff and erosion, *Catena*, *67*(1), 68–78, doi:10.1016/j.catena.2006.03.002.

Parsons, A. J., A. D. Abrahams, and J. Wainwright (1996), Responses of interrill runoff and erosion rates to vegetation change in southern Arizona, *Geomorphology*, *14*, 311–317, doi:10.1016/0169-555X(95)00044-6.

Parsons, A. J., J. Wainwright, W. H. Schlesinger, and A. D. Abrahams (2003), The role of overland flow in sediment and nitrogen budgets of mesquite dunefields, southern New Mexico, *J. Arid Environ.*, *53*(1), 61–71, doi:10.1006/jare.2002.1021.

Ravi, S., P. D'Odorico, and G. S. Okin (2007), Hydrologic and aeolian controls on vegetation patterns in arid landscapes, *Geophys. Res. Lett.*, *34*(24), L24S23, doi:10.1029/2007GL031023.

Schlesinger, W. (1985), The formation of caliche in soils of the Mojave Desert, California, *Geochim. Cosmochim. Acta*, *49*, 57–66, doi:10.1016/0016-7037(85)90191-7.

Schlesinger, W. H., J. F. Reynolds, G. L. Cunningham, L. F. Huenneke, W. M. Jarrell, R. A. Virginia, and W. G. Whitford (1990), Biological feedbacks in global desertification, *Science*, *247*(4946), 1043–1048, doi:10.1126/science.247.4946.1043.

Schlesinger, W. H., J. A. Raikes, A. E. Hartley, and A. E. Cross (1996), On the spatial pattern of soil nutrients in desert ecosystems, *Ecology*, *77*(2), 364–374, doi:10.2307/2265615.

Schlesinger, W. H., A. D. Abrahams, A. J. Parsons, and J. Wainwright (1999), Nutrient losses in runoff from grassland and shrubland habitats in Southern New Mexico: I. rainfall simulation experiments, *Biogeochemistry*, *45*(1), 21–34, doi:10.1007/BF00992871.

Schlesinger, W. H., T. J. Ward, and J. Anderson (2000), Nutrient losses in runoff from grassland and shrubland habitats in southern New Mexico: II. Field plots, *Biogeochemistry*, *49*(1), 69–86, doi:10.1023/A:1006246126915.

Stein, R. A., and J. A. Ludwig (1979), Vegetation and soil patterns on a Chihuahuan Desert bajada, *Am. Midl. Nat.*, *101*, 28–37, doi:10.2307/2424898.

Turnbull, L., J. Wainwright, and R. E. Brazier (2008), A conceptual framework for understanding semi-arid land degradation: Ecohydrological interactions across multiple-space and time scales, *Ecohydrology*, *1*(1), 23–34, doi:10.1002/eco.4.

Turnbull, L., J. Wainwright, and R. E. Brazier (2010), Hydrology, erosion and nutrient transfers over a transition from semi-arid grassland to shrubland in the South-Western USA: A modelling assessment, *J. Hydrol.*, *388*(3–4), 258–272, doi:10.1016/j.jhydrol.2010.05.005.

Turnbull, L., J. Wainwright, and R. E. Brazier (2011), Nitrogen and phosphorus dynamics during runoff events over a transition from grassland to shrubland in the south-western United States, *Hydrol. Processes*, *25*(1), 1–17, doi:10.1002/hyp.7806.

Wainwright, J. (2006), Climate and climatological variations, in *Structure and Function of a Chihuahuan Desert Ecosystem: The Jornada Basin Long-Term Ecological Research Site*, edited by K. Havstad et al., pp. 36–97, Oxford Univ. Press, Oxford.

Wainwright, J. (2009), Desert ecogeomorphology, in *Geomorphology of Desert Environments*, edited by A. J. Parsons and A. D. Abrahams, pp. 21–66, Springer, Berlin, doi:10.1007/978-1-4020-5719-9_3.

Wainwright, J., A. J. Parsons, and A. D. Abrahams (2000), Plot-scale studies of vegetation, overland flow and erosion interactions: Case studies from Arizona and New Mexico, *Hydrol. Processes*, *14*(16–17), 2921–2943, doi:10.1002/1099-1085(200011/12)14:16/17<2921::AID-HYP127>3.0.CO;2-7.

Wainwright, J., A. J. Parsons, W. H. Schlesinger, and A. D. Abrahams (2002), Hydrology-vegetation interactions in areas of discontinuous flow on a semi-arid bajada, Southern New Mexico, *J. Arid Environ.*, *51*(3), 319–338, doi:10.1006/jare.2002.0970.

Whitford, W. G. (2002), *Ecology of Desert Systems*, Elsevier Sci., London.

Yao, J., D. P. C. Peters, K. M. Havstad, R. P. Gibbens, and J. E. Herrick (2006), Multiscale factors and long-term responses of Chihuahuan Desert grasses to drought, *Landscape Ecol.*, *21*, 1217–1231, doi:10.1007/s10980-006-0025-8.